Electronic Supplementary Material (ESI) for Journal of Materials Chemistry A.

Electronic Supplementary Information (ESI)

A Polymer-Coated Carbon Black-based Fuel Cell Electrocatalyst with High CO-Tolerance and Durability in Direct Methanol Oxidation

Zehui Yang[a], Mohamed R. Berber[b,d], and Naotoshi Nakashima*[a,b,c]

[a] *Department of Applied Chemistry, Graduate School of Engineering, Kyushu University, 744 Motooka Nishi-ku, Fukuoka 819-0395, Japan*

[b] *International Institute for Carbon-Neutral Energy Research (WPI-I2CNER), Kyushu University, 744 Motooka Nishi-ku, Fukuoka 819-0395, Japan*

[c] *JST-CREST, 5 Sanbancho, Chiyoda-ku, Tokyo, 102-0075, Japan*

[d] *Department of Chemistry, Faculty of Science, Tanta University, Tanta 31527, Egypt*

*E-mail: nakashima-tcm@mail.cstm.kyushu-u.ac.jp

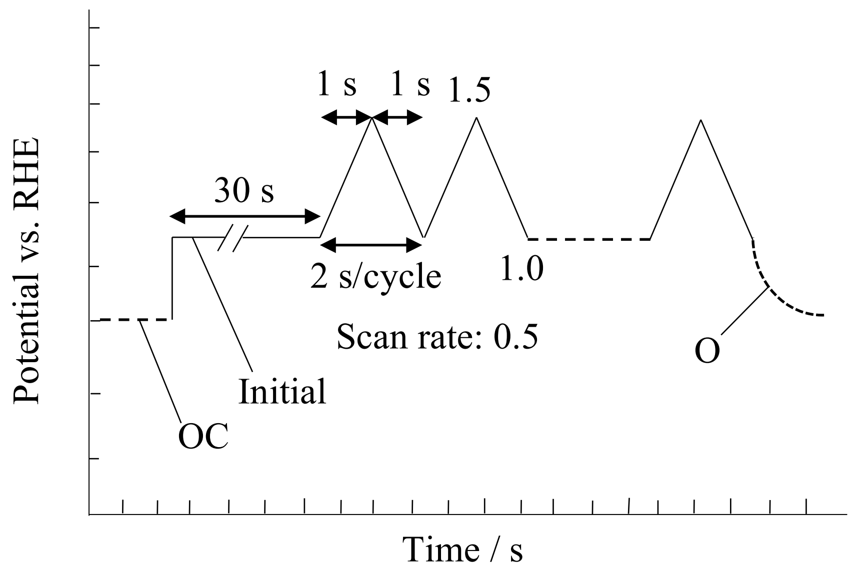

Fig. S1. New test protocol of durability test for a half-cell proposed by the Fuel Cell Commercialization Conference of Japan (see K. Shinohara, A. Ohma, A. Iiyama, T. Yoshida and T. Daimaru, *ECS Transactions*, 2011, **41**, 775).

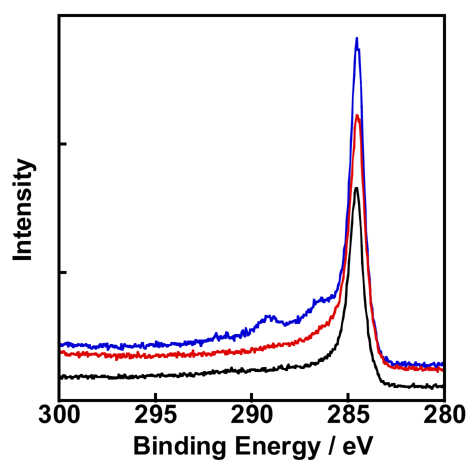

Fig. S2. The narrow scan of C_{1s} region of CB/Pt (black line), CB/PyPBI/Pt (blue line) and CB/PyPBI/Pt/PVPA (red line).

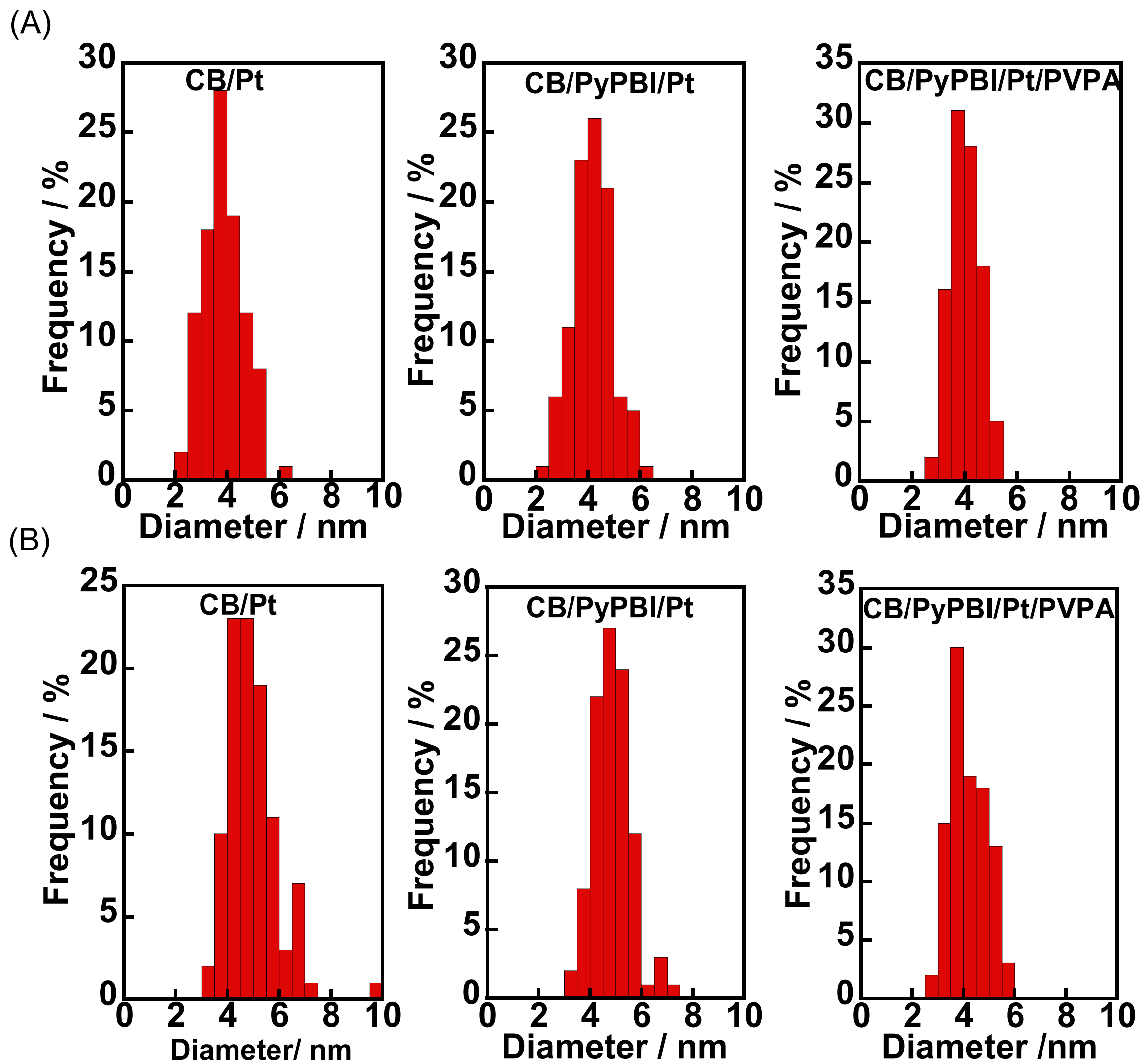

Fig. S3. Histograms of the particle size distribution of CB/Pt, CB/PyPBI/Pt and CB/PyPBI/Pt/PVPA before (top column A) and after (bottom column B) the durability test. To present the histograms, 100 nanoparticles were taken from each TEM image.

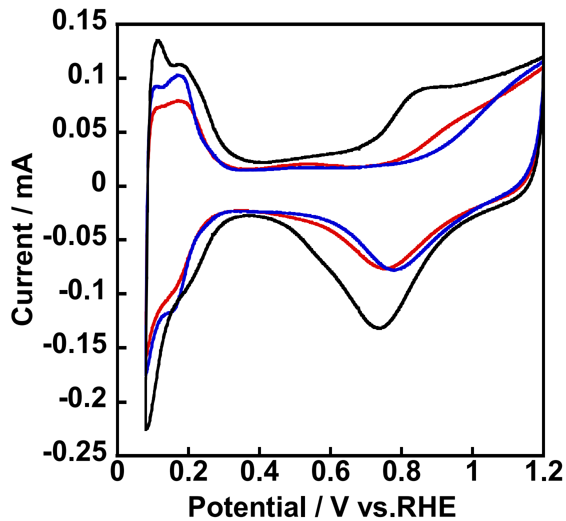

Fig. S4. CV curves of CB/Pt (black line), CB/PyPBI/Pt (blue line), and CB/PyPBI/Pt/PVPA (red line) recorded in 0.1M $HClO_4$ solution at the scan rate of 50 mV/s at 25 ˚C.

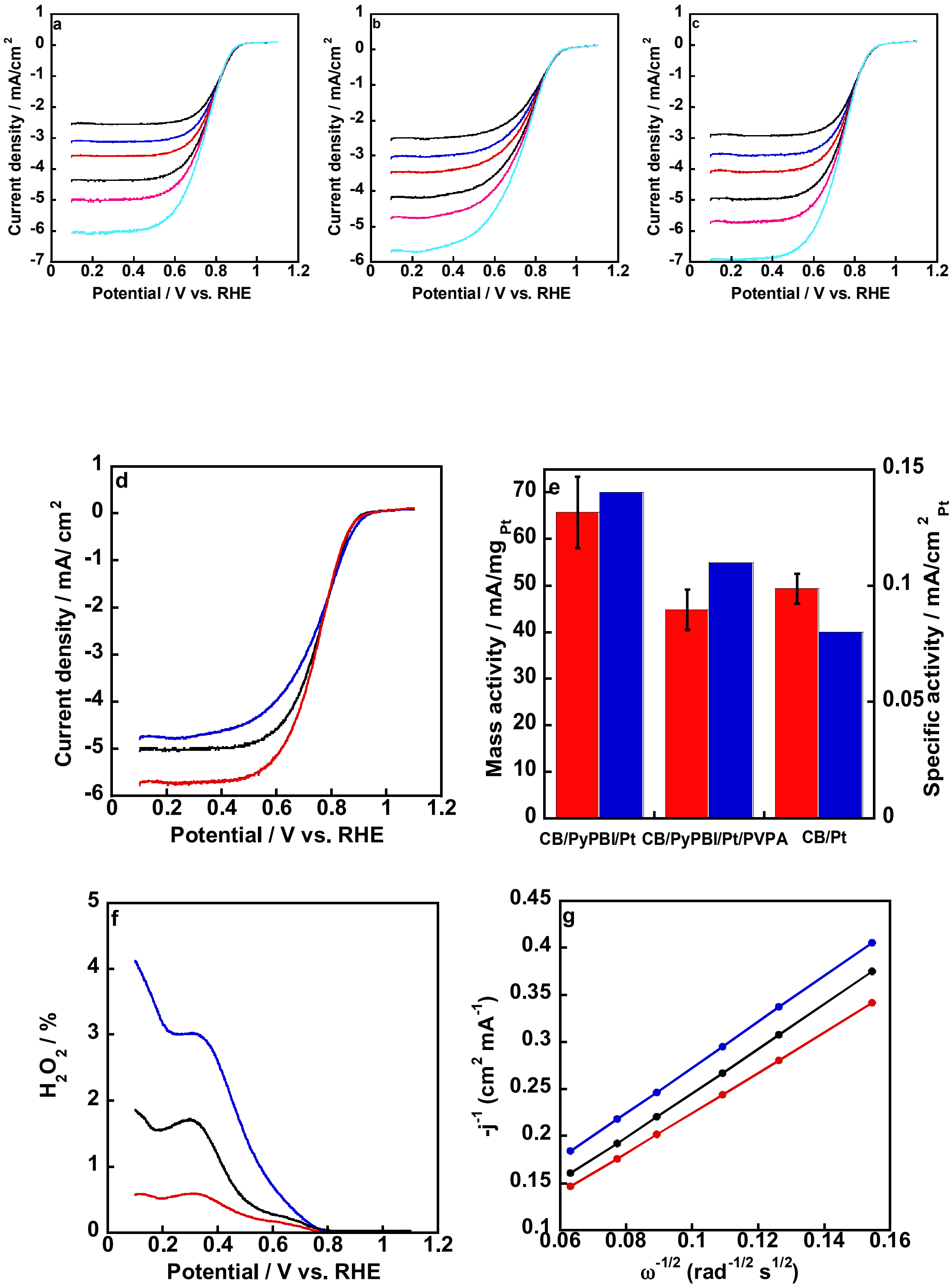
a
b
c
d
e
f
g
Current density / mA/cm^2
Potential / V vs. RHE
Current density / mA/ cm^2
Mass activity / mA/mg$_{Pt}$
Specific activity / mA/cm^2$_{Pt}$
CB/PyPBI/Pt
CB/PyPBI/Pt/PVPA
CB/Pt
H_2O_2 / %
$-j^{-1}$ (cm^2 mA^{-1})
$\omega^{-1/2}$ (rad$^{-1/2}$ s$^{1/2}$)

Fig. S5. Rotating disc current density of CB/Pt (a), CB/PyPBI/Pt (b) and CB/PyPBI/Pt/PVPA (c) in O_2-saturated 0.1M $HClO_4$ solutions at 25 ˚C. (d) ORR polarization curves for CB/Pt (black line), CB/PyPBI/Pt (blue line), and CB/PyPBI/Pt/PVPA (red line) in O_2-saturated 0.1M $HClO_4$ at 25 ˚C and rotation rate of 1600 rpm, sweep rate of 10 mV/s. (e)Mass (red column) and specific activities (blue column) at 0.85 V *vs*. RHE (N=3). (f) Peroxide generation from the ORR detected at ring electrode in O_2-saturated 0.1M $HClO_4$ at sweep rate of 10 mV/s, and rotation rate of 1600 rpm. (g) Koutecky-Levich plots from ORR at 0.43 V *vs*. RHE for CB/Pt (black line), CB/PyPBI/Pt (blue line), and CB/PyPBI/Pt/PVPA (red line).

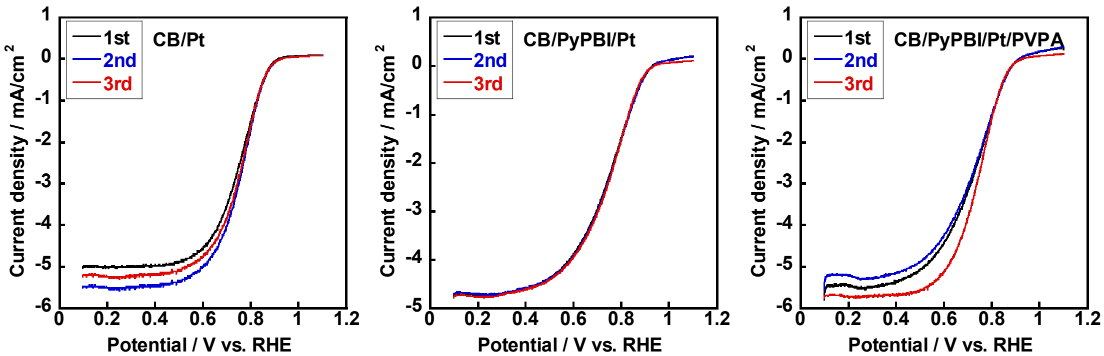

Fig. S6. Three ORR polarization curves for CB/Pt, CB/PyPBI/Pt, and CB/PyPBI/Pt/PVPA in O_2-saturated 0.1M $HClO_4$ at 25 ˚C and rotation rate of 1600 rpm, sweep rate of 10 mV/s.

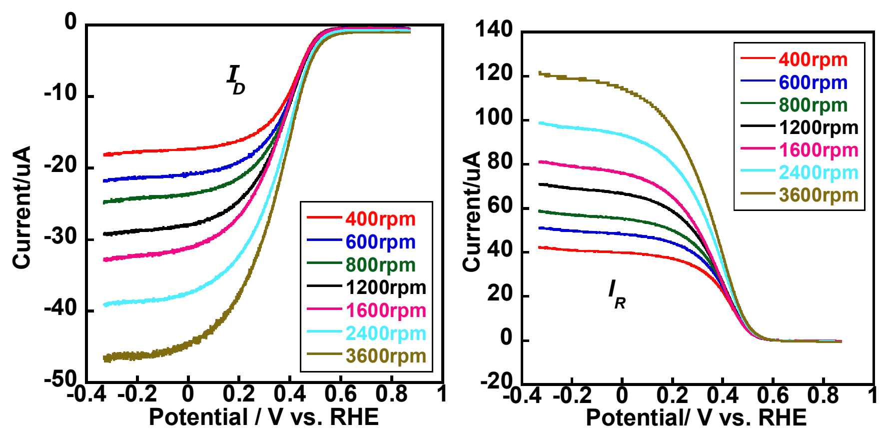

Fig. S7. Ring (I_R) and disk currents (I_D) for the collection efficiency in N_2-saturated 0.1M KCl and 1mM $K_3Fe(CN)_6$ at the scan rate of 10 mV/s at 25˚C.

Explanation of Fig. S5, 6 and 7: Before the durability test, the ORR was measured (Fig. S5†). Interestingly, after coating with PVPA, the CB/PyPBI/Pt PVPA showed a higher limiting disk current (-5.77mA/cm^2) than the other two catalysts because of the perfect oxygen accessibility, which contributed to a higher fuel cell performance of the PVPA coated catalyst.[1] The mass and specific activities were calculated as a quantitative comparison to illustrate the performance of all catalysts using the Levich-Koutecky equation: $1/i=1/i_k+1/i_d$.[2] Three-times ORR measurements were carried out for each catalyst to calculate the average mass and specific activities (Fig. S6†). Compared to the CB/PyPBI/Pt (65.70 mA/mg_{Pt} and 0.14 mA/cm^2_{Pt}, respectively), the mass and specific activities of the CB/PyPBI/Pt/PVPA decreased due to coverage of the polymer layer on the Pt-NPs (44.72 mA/mg_{Pt} and 0.11 mA/cm^2_{Pt}, respectively). However, the value was almost the same as that of the commercial CB/Pt (49.33 mA/mg_{Pt} and 0.08 mA/cm^2_{Pt}, respectively) (Fig. S5e†). During the ORR, peroxide (H_2O_2) is generated as a by-product, which degrades the performance by deterioration of the Pt-based anode and carbon supporting materials. Thus, a lower H_2O_2 yield is very important for the catalyst durability. After being coated by PVPA, the H_2O_2 generation, which was calculated by the equation: $\%H_2O_2=200I_R/(NI_D+I_R)$, where N is the collection efficiency, which corresponds to the I_R/I_D ratio (0.404, Fig. S7†), significantly decreased to 0.6 % (Fig. S5f†) attributed to the 4-electron transfer during the ORR (Fig. S5g†).

Table S1. Comparison of mass activity in methanol oxidation reaction (MOR).

Catalysts	Mass activity (mA/mg)	Methanol concentration (mol/L)	Ref.
CB/PyPBI/Pt/PVPA	817	1	this work
PtRu/MC	487.9	1	3
PtRu/graphene	205.7	1	4
PtRu/graphene	33.5	2	5
PtRu/CNT/graphene	136.7	1	6
PtRu/TiO_2/CNF	516	2	7
PtRu/PANI/CNT	622.7	1	8
PtRu/PEI/CNT	636	1	9
PtRu/HPAs-CS/graphene	232	1	10
PtRu/N-doped graphene	668	0.5	11

References

1 M. R. Berber, T. Fujigaya and N. Nakashima, *ChemcatChem*, 2014, **6**, 567.

2 H. W. Liang, X. Cao, F. Zhou, C. H. Cui, W. J. Zhang and S. H. Yu, *Adv. Mater.*, 2011, **23**, 1467.

3 T. Maiyalagan, T. O. Alaje and K. Scott, *J. Phy. Chem. C*, 2012, **116**, 2630.

4 J. Zhao, L. Zhang, H. Xue, Z. Wang and H. Hu, *RCS adv.*, 2012, **2**, 9651.

5 C. Nethravathi, E. A. Anumol, M. Rajamathi and N. Ravishankar, *Nanoscale*, 2011, **3**, 569.

6 Y.-S. Wang, S.-Y. Yang, S.-M. Li, H.-W. Tien, S.-T. Hsiao, W.-H. Liao, C.-H. Liu, K.-H. Chang, C.-C. M. Ma and C.-C. Hu, *Electrochim. Acta*, 2013, **87**, 261.

7 Y. Ito, T. Takeuchi, T. Tsujiguchi, M. A. Abdelkareem and N. Nakagawa, *J. Power Sources*, 2013, **242**, 280.

8 H.-Y. Lee, W. Vogel and P. P.-J. Chu, *Langmuir*, 2011, **27**, 14654.

9 Y. Cheng and S. P. Jiang, *Electrochim. Acta*, 2013, **99**, 124.

10 Z. Cui, C. M. Li and S. P. Jiang, *Phys. Chem. Chem. Phys.*, 2011, **13**, 16349.

11 S. Zhao, H. Yin, L. Du, G. Yin, Z. Tang and S. Liu, *J. Mater. Chem. A*, 2014, **2**, 3719.